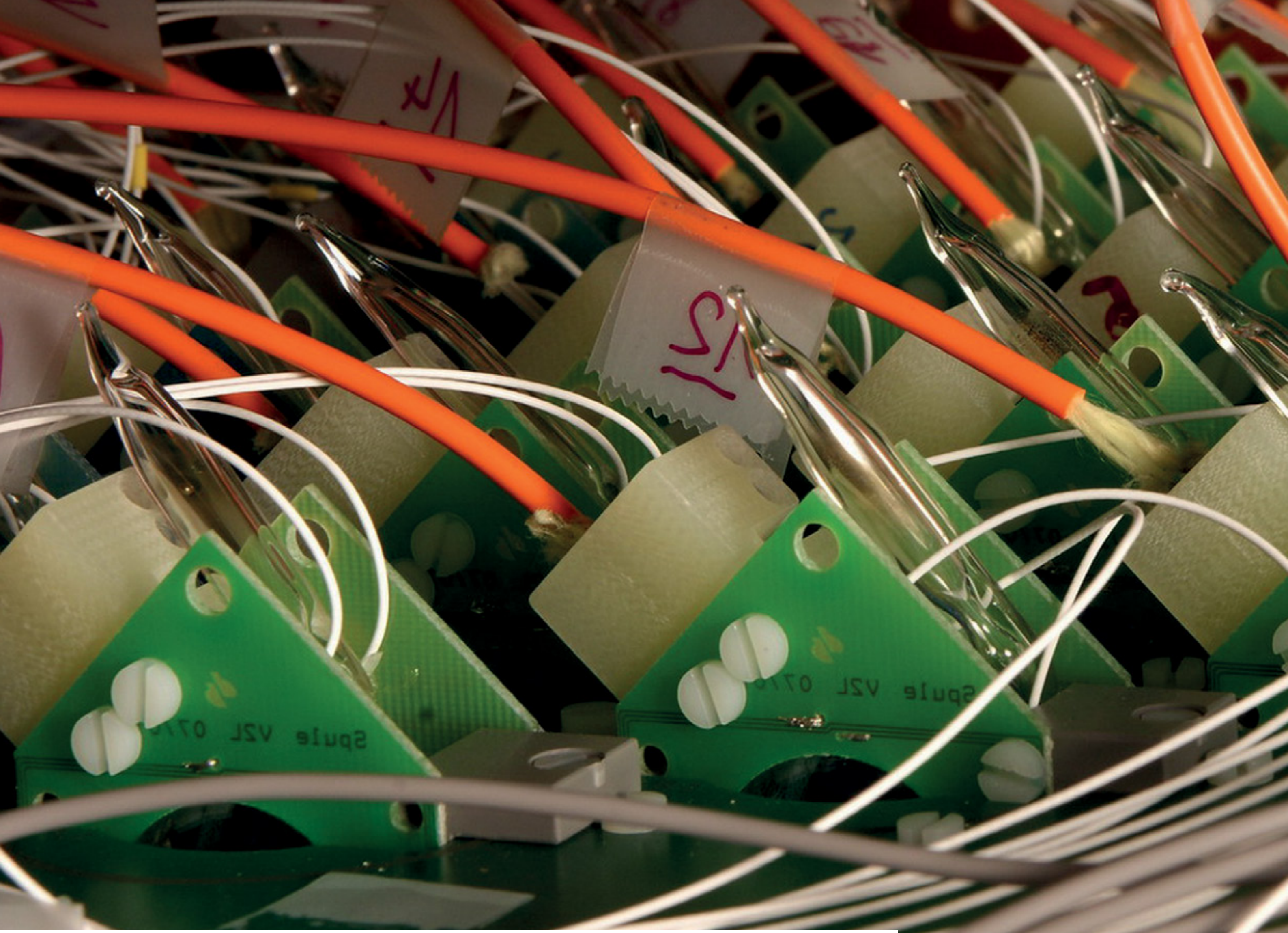

Optically pumped alkali
magnetometers for biomedical applications

■ **Antoine Weis** - Physics Department, University of Fribourg, Switzerland - antoine.weis@unifr.ch - DOI: 10.1051/epn/2012301

Atomic magnetometers are novel sensitive devices for medical diagnosis. They use laser radiation to prepare spin-coherent atomic samples and to monitor their perturbation by the magnetic field of interest [1]. In recent years, they have reached sensitivities comparable to [2], or better than [3] SQUID magnetometers. We discuss the principles of atomic magnetometers based on optically detected magnetic resonance (ODMR) and review their biomedical applications.

▲ Partial view of sensor array in the 19-channel Fribourg magnetocardiography (MCG) device and (inset) subject positioned for MCG measurements (Details in the text).

Optically pumped atomic magnetometers measure the Larmor frequency ν_L at which the bulk magnetization of a spin-polarized alkali metal vapour in a glass cell precesses around the field of interest $\vec{B}_0$. The precession frequency is related to the modulus of the magnetic field by $\nu_L=(\gamma/2\pi)|\vec{B}_0|$, where $\gamma/2\pi\approx3.5$Hz/nT for ^{133}Cs, so that the magnetic field measurement consists in a frequency measurement. In so-called ODMR magnetometers, ν_L is determined by Optically Detected Magnetic Resonance using laser radiation.

The general principle of an ODMR magnetometer can be understood as follows: A bulk spin polarization is created in the atomic medium through optical pumping, a process introduced in the 1950s, by which angular momentum of polarized light, resonant with an atomic

Article available at http://www.europhysicsnews.org or http://dx.doi.org/10.1051/epn/2012301

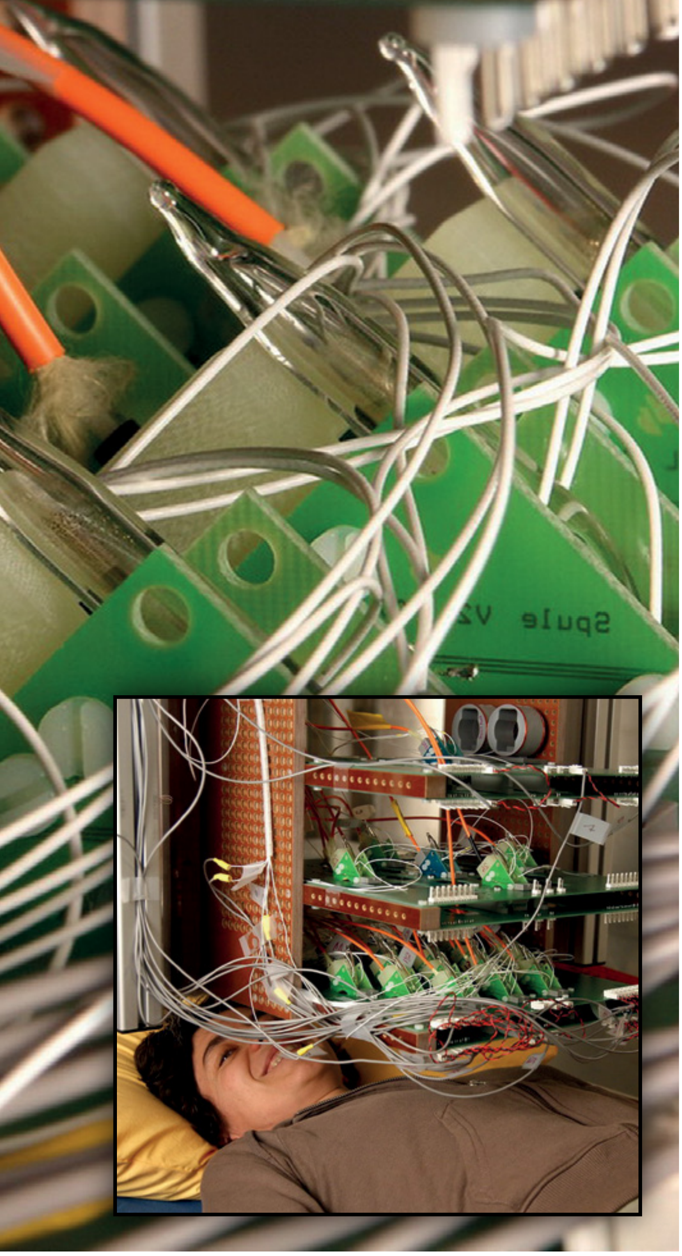

absorption line, is transferred to the atomic medium by multiple absorption-emission cycles. With circularly polarized light, the medium acquires in this way a vector magnetization – called orientation –, while linearly polarized light produces a tensor magnetization – called alignment. Here we consider only vector polarization $\vec{S}$ and the associated bulk vector magnetization $\vec{M} \propto \vec{S}$. The (suitably oriented) magnetic field $\vec{B}_0$ exerts a torque on $\vec{M}$, which induces its precession around $\hat{B}_0$. This precession – together with spin relaxation – produces a steady-state magnetization, whose direction and magnitude differ from the magnetization initially created by optical pumping. Detection relies on the fact that the optical absorption coefficient of a spin-polarized atomic medium depends on the magnitude and orientation of its magnetization. The alterations of the magnetization by the magnetic field can therefore be probed by recording the transmitted light power. In the simplest realization of an ODMR magnetometer, a single light beam serves both to prepare and to probe the magnetization.

Modern Optically Pumped Magnetometers (OPMs) use narrowband laser light, whose frequency is stabilized to a specific absorption line of the atomic medium. They use a coherent drive (modulation) mechanism for synchronizing the spin precession initiated by optical pumping. The drive at frequency ν_{mod} leads to a modulation of the transmitted light intensity, whose amplitude and phase are extracted by phase-sensitive (lock-in) detection. The various modulation techniques deployed for the phase-synchronous drive of the spins distinguish between the growing number of magnetometer types known today.

In the ODMR magnetometer (Figure 1, left) the synchronizing coherent drive is provided by an additional weak magnetic field oscillating (or rotating) at the frequency ν_{mod}. The amplitude and phase relations between the drive and the magnetometer response in terms of the transmitted intensity modulation, are those of a classical harmonic oscillator: the amplitudes of the in-phase and quadrature components have a resonant dispersive and absorptive Lorentzian dependence, respectively, on the detuning $\delta\nu = \nu_{mod} - \nu_L$, while the phase ϕ between drive and response has an arctan-dependence on $\delta\nu$ (Figure 1, right). The near-resonance linear dependence of the dispersive signal or the phase signal on $\delta\nu$ is used in an electronic feedback loop that ensures that the drive frequency ν_{mod} tracks the Larmor frequency ν_L in a phase-coherent manner: ν_{mod} then carries the magnetometric information. The magnetometric sensitivity is determined by the ratio of the resonance linewidth and the signal-to-noise ratio (SNR) of the optical detection. Narrow resonances must ensure long spin coherence relaxation times, made possible by preventing spin depolarization due to collisions with the cell walls. This is achieved in our magnetometers by a polarization-preserving wall coating [4] (other magnetometers use inert buffer gases to slow down wall collisions). The ODMR magnetometers are operated near the shot noise limit of the detection light with a SNR (in a 1 Hz bandwidth) in excess of 10^5, yielding intrinsic sensitivities of a few 10 $fT/Hz^{1/2}$, or below [2].

Biomedical applications

ODMR magnetometer detection of cardiomagnetic fields

The magnetic field of the beating human heart is the strongest field of medical interest, albeit more than a

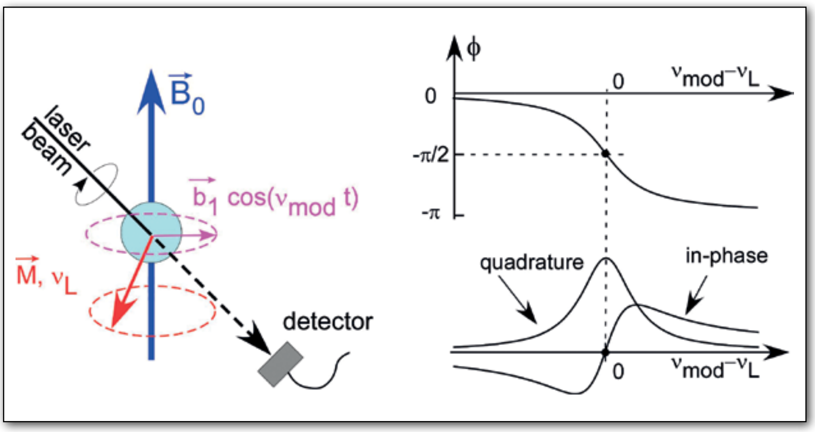

▼ **FIG. 1:** Left: In the ODMR-magnetometer, the transmitted light intensity is modulated when the rotating (oscillating) weak drive field b_1 is synchronized to the precessing magnetization $\vec{M}$. Right: Signals extracted by phase-sensitive detection. The dots mark the working point that is established by electronic feedback.

million times weaker than the (weak) geomagnetic field. A magnetocardiogram (MCG) is a representation of the time dependence of the out-of-chest component of the cardiac magnetic field during one period of the cardiac cycle. For measuring MCG signals, fluctuating environmental magnetic fields and their gradients have to be suppressed by appropriate shielding in combination with first- or second-order differential measurements involving two or three sensors, respectively. In practice, the ambient field is cancelled and an offset field of a few percent of the earth field is applied perpendicular to the subject's chest, so that the magnetometer(s) oscillate at the corresponding Larmor frequency. The projection of the magnetic field from the heart onto the direction of the offset field modifies the Larmor frequency and this modification represents the actual MCG signal.

In 2003, we could show for the first time that MCG signals can be detected by two laser-driven OPMs forming a first-order gradiometer [5]. By moving the subject with respect to the magnetometers we were able to record two-dimensional maps of the magnetic field distribution from the heart [6]. Cardiomagnetic map dynamics during the QRS-complex and the T-wave can be seen as animations in [6]. These early measurements were done in a μ-metal shielding room, where the subject had to lie still during the 2 hours required to record all data for the animations. In a subsequent multi-year effort we have developed a 25-sensor array [7] which allows us to infer dynamic maps from the simultaneous recording of MCG signals at 19 positions over the chest (see Fig. 2). This brought the measurement time down to less than 2 minutes.

A close-up view of the apparatus used to record the signals of Fig. 2 is shown in the introductory illustration, where one sees a sub-ensemble of the 25 identical compact magnetometer modules, in which the geometry of Fig. 1 is implemented. An optical fibre (orange) brings the light to the module, in which the circularly polarized beam traverses the vapour cell, after which it is detected by a photodiode. The field $\vec{b}_1(t)$ is produced by two coils laid out on the (green) printed circuit boards. The (white) coaxial cables bring the current to these coils and carry the photocurrent to the electronics. The system is operated by a complex system [7] of phase-sensitive detectors and electronic feedback loops controlled by a digital field-programmable gate array system. In view of potential hospital installations we performed these measurements in a double-walled aluminium shielding room which provides sufficient suppression of magnetic fields oscillating at the line frequency.

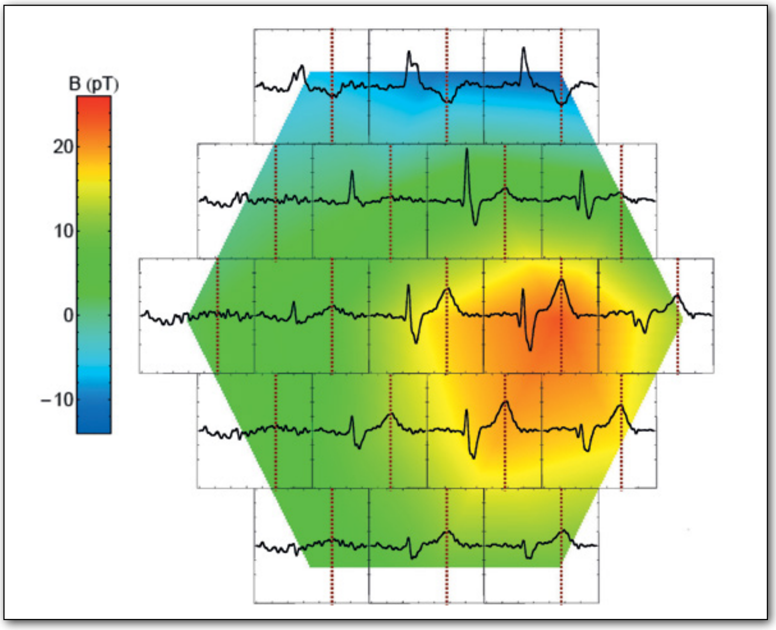

▼ **FIG. 2:** Magnetocardiogram (MCG) map of the human heart. The individual graphs represent 19 denoised MCG traces recorded by a hexagonal array of 19 atomic magnetometers (see title figure) spaced by 50 mm, and located 25 mm above the chest. The magnetic field values at the times marked by the vertical dotted red lines (T-wave) were used to construct the underlying map by interpolation [9].

Alternative schemes for MCG detection

Since our first demonstration of MCG detection by laser-pumped atomic magnetometers in 2003, a growing number of research teams have joined the field. In 2007, MCG traces were recorded in an unshielded environment using a magnetometer based on frequency modulation [8]. More recently, MCG detection by chip-scale ODMR magnetometers was compared to SQUID-based detection in the high performance magnetic shielding room at PTB-Berlin [9]. Spin-exchange relaxation free magnetometers [3] have been applied for recording magneto-encephalographic signals [10], and have recently produced human [11] and fetal [12] MCG signals of outstanding quality.

Discussion

The noninvasive and contact-free detection of cardiomagnetic fields has a high potential for the early detection of cardiovascular diseases, which themselves represent the most common cause of death in industrialized countries. MCG maps allow, *e.g.*, the localization of abnormal current sources in the myocardium related to arrhythmias and other heart conditions. Source localization from measured magnetic field distributions (the so-called inverse problem) profits from the fact that the magnetic fields – in contrast to the electric fields detected in standard ECG signals – are not perturbed by the tissue between the heart and the detector.

However, more than 40 years after the first recording of MCG signals by liquid He-cooled SQUID magnetometers, the method of MCG diagnostics has not yet found a way into every-day clinical practice. There is hope that atomic magnetometers operated at room temperature will help to change this situation.

Outlook

Atomic magnetometers are about to find another promising application in the field of biomedical imaging. The method relies on the detection of the magnetic field produced by magnetic nanoparticles (MNP) [9]. Since a few years, such particles are being used in medical applications, such as drug delivery, hyperthermic therapy, MRI contrast enhancement, and medical imaging. The latter application uses MNPs embedded in functionalized shells that preferentially attach to (or are taken up by) specific biological entities such as organs, tumors, or cells. The relaxation time of the magnetization of bound MNPs surpasses that of unbound particles by orders of magnitude. The spatial mapping of these relaxation times, monitored by recording the corresponding magnetic field decays with OPMs thus opens new ways for the imaging of organs and tumors. The technique is known as magneto-relaxometry (MRX). We are currently investigating MRX signals from super-paramagnetic iron oxide nanoparticles (Fig. 3) using the apparatus described in [7].

Conclusion

Although OPMs have been around for more than half a century, the advent of affordable tunable laser sources has opened new perspectives for atomic magnetometry, as witnessed by the growing number of novel magnetometric techniques developed in the past decade. For many applications, OPMs have the potential to replace cryogenic SQUID detectors which have been for a long time the undisputed kings in low-field magnetometry, and in biomedical applications. ■

About the author

Antoine Weis received a Ph. D. degree in physics (1984) from ETH Zurich. He worked at MPI for Quantum Optics (Garching) and was Associate Professor at the University of Bonn. Since 1999 he holds the Chair for Atomic Physics at the University of Fribourg. His work on biomagnetometry has been honoured by an Innovation Award from the Wall Street Journal Europe in 2003 and has been nominated for the Leibinger Innovationspreis in 2004.

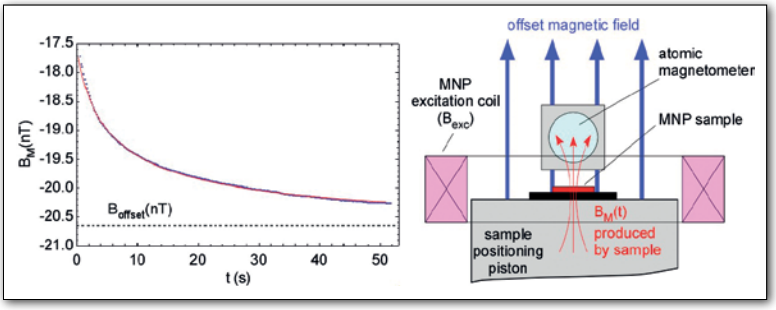

▲ **FIG. 3.** Magneto-relaxation signal from super-paramagnetic nanoparticles containing 5 mg of iron following a several seconds long magnetization in a field B_{exc} of 5 mT (unpublished).

Acknowledgements

The MCG project would not have been possible without a generous grant from the Velux Foundation. The nanoparticle project is supported by a Sinergia grant (CRSII2 130414) from the Swiss National Science Foundation.

References

[1] A recent comprehensive review of the field was given by D. Budker, *M. Romalis in Nature Physics* **3**, 227 (2007).

[2] S. Groeger, J.-L. Schenker, R. Wynands, A. Weis, *Eur. Phys. J. D* **38**, 239 (2006).

[3] I. K. Kominis, T. W. Kornack, J. C. Allred, M. V. Romalis, *Nature* **422**, 596 (2003).

[4] N. Castagna, G. Bison, G. Di Domenico, A. Hofer, P. Knowles, C. Macchione, H. Saudan, A. Weis, *Appl. Phys. B* **96**, 763 (2009).

[5] G. Bison, R. Wynands, A. Weis, *Appl. Phys. B* **76**, 325 (2003).

[6] G. Bison, R. Wynands, A. Weis, *Opt. Expr.* **11**, 904 (2003).

[7] G. Bison, N. Castagna, A. Hofer, P. Knowles, J.-L. Schenker, M. Kasprzak, H. Saudan, A. Weis, *Appl. Phys. Lett.* **95**, 173701 (2009).

[8] J. Belfi, G. Bevilacqua, V. Biancalana, S. Cartaleva, Y. Dancheva, L. Moi, *JOSA B* **24**, 2357 (2007) .

[9] S. Knappe, T. H. Sander, O. Kosch, F. Wiekhorst, J. Kitching, L. Trahms, *Appl. Phys. Lett.* **97**, 133703 (2010).

[10] H. Xia, A. Ben-Amar Baranga, D. Hoffman, M.V. Romalis, *Appl. Phys. Lett.* **89**, 211104 (2006).

[11] R. Wyllie, M. Kauer, G.S. Smetana, R.T. Wakai, T.G. Walker, *Phys. Med. Biol.* **57**, 2619 (2012)

[12]. R. Wyllie, M. Kauer, R. T. Wakai, T. G. Walker, arXiv:1202.5019v1 (2012).

LETTER TO THE EDITORS

Comments on the article on wind energy of C. le Pair *et al.* in Europhysics News 43/2, 22

The authors state "quantifying the efficiency (of wind energy) ... is by no means a simple matter." As true as this is, however, they present many simplifications to show the unsuitability of wind power as a large-scale energy provider. Besides several wrong statements, our major concern is the complete neglect of the fact that the current energy system is in a strongly transitional phase. Any analysis based on yesterday's configuration of power plant mix, transmission and distribution, and load management cannot contribute much significant insight into possibilities of future energy systems. It is state of the art to consider different types of energy producers, trans-national transport of energy, forecasting and diversification methods, demand side management, and so on. The challenge is to transform an old inflexible power system into a new complex and adaptive one. The insights obtained from the physics of complex systems have shown that, based on a deep understanding of the interaction of dynamic subsystems, intelligent coupling and control are required to achieve an efficient overall performance. This implies that a simple rigid coupling will lead to efficiency losses like those complained by the authors.

■ **J. Peinke and D. Heinemann,**
Institute of Physics, Uni Oldenburg